A tunable universal terahertz filter using artificial dielectrics based on parallel-plate waveguides

Rajind Mendis,[a] Abhishek Nag, Frank Chen,[b] and Daniel M. Mittleman
Department of Electrical and Computer Engineering, Rice University, MS-366, 6100 Main Street, Houston, Texas 77005, USA

(Received 23 August 2010; accepted 10 September 2010; published online 29 September 2010)

Using parallel-plate waveguides (PPWGs) that mimic artificial dielectrics, we demonstrate a universal filter that provides low-pass, high-pass, band-pass, and band-stop (or notch) filtering functionalities in the terahertz (THz) frequency regime. The device essentially consists of two PPWGs in a complementary geometry. The filtering functionality is achieved by positioning an appropriate amplitude mask in the path of the spatially chirped THz beam between the two waveguides. By varying the position of the mask, we experimentally and theoretically demonstrate continuous tunability of the respective 3 dB cutoff frequencies within the frequency range from about 0.3 to 0.7 THz. © *2010 American Institute of Physics*. [doi:10.1063/1.3495994]

In recent years, there has been a growing interest in applications of terahertz (THz) radiation. This interest has highlighted the need for numerous functional devices and components for controlling and manipulating THz waves, many of which are still lacking. For broadband THz systems, one such component is a tunable filter. Spectral filtering is a key capability in many different optical systems, and will be crucial in the implementation of future broadband THz communications systems.[1]

Spectral filters for free-space THz beams have been the topic of many studies in recent years. The simplest example, a circular aperture placed at the focus (or waist) of a broadband THz beam, acts as a high-pass filter (HPF) with a cutoff frequency controlled by the aperture diameter.[2] However, other common filtering functions, such as low-pass, band-pass, and band-stop filtering, are harder to implement, especially if one requires dynamic control of filter parameters. Various concepts based on photonic crystals, frequency-selective surfaces, metamaterials, or liquid crystals have been described.[3–8] Here, we describe a *universal* THz filter, capable of providing low-pass, high-pass, band-pass, and band-stop (or notch) filtering functionalities, along with continuous tunability of the filter's cutoff frequency/ies.

Our filter design exploits the characteristic frequency dependence in the phase velocity of the lowest-order transverse-electric (TE_1) mode[9,10] of the parallel-plate waveguide (PPWG).[11] Recently, we have shown that this frequency dependence can be used as the basis for a two-dimensional artificial dielectric medium with an effective refractive index of $0 \leq n < 1$.[12] Here, we engineer this spectral dispersion so that a THz wave propagating inside the waveguide refracts as in a conventional dielectric prism, although in this case we have a greater degree of control over the dispersion. In fact, this device concept would allow exclusive spatial access to every frequency component contained within a broadband THz pulse.

The experimental device geometry consists of two complementary PPWGs as shown in Fig. 1(a). The THz beam is coupled into $PPWG_1$ at oblique incidence, polarized to excite the TE_1 mode of the waveguide. Because different frequency components experience different refractive indices inside the waveguide, Snell's law dictates that the direction of propagation inside the waveguide is frequency dependent. Since the refractive index varies monotonically from unity to zero as the frequency decreases,[12] the beam exiting $PPWG_1$ is *spatially chirped*: the high-frequency components lie closer to the input optic-axis (indicated by blue) and the low-frequency components are displaced from the optic-axis (indicated by red). The spatially-spread beam is then coupled into an identical $PPWG_2$, which is in a complementary geometry. This reverses the spatial chirp, combining the different frequency components back into a single output beam. By choosing the proper plate separation, waveguide length, and angular positioning, we can carry out various spectral filtering functions simply by blocking portions of the spatially chirped beam between the two waveguides.

We demonstrate a tunable low-pass filter (LPF) by positioning a metal plate centrally between the two PPWGs, and moving it perpendicularly into the path of the beam starting from the input optic-axis end [see Fig. 1(a)]. As the plate moves in, it blocks (or filters) frequency components starting from the high-end of the input spectrum, effectively realizing a LPF whose upper-cutoff frequency can be tuned by varying the position of the plate. Figure 1(b) shows typical time-domain output signals as the plate moves in by 3 and 5 mm from an unblocked (reference) position. All three signals show a negative chirp characteristic of the TE_1 mode, with high-frequency components arriving earlier in time. This *temporal* chirp allows us to observe a progressive decrease in amplitude starting from the high-frequency end, when the plate moves in, as expected for a LPF. The corresponding spectra shown in Fig. 1(c) confirm the low-pass behavior.

We can extract the filter response [inset of Fig. 1(d)] by normalizing the output spectra to the reference spectrum. The frequency at which the amplitude transmission drops to 70% gives the experimental value of the 3 dB (half-power) cutoff frequency. The theoretical value of the cutoff frequency can be derived by calculating the frequency-dependent lateral shift in the optic axis of the THz beam between the waveguides. We chose a 1 mm plate separation,

[a]Electronic mail: rajind@rice.edu.
[b]Present address: Department of Electrical Engineering, Stanford University, Stanford, California 94305, USA.

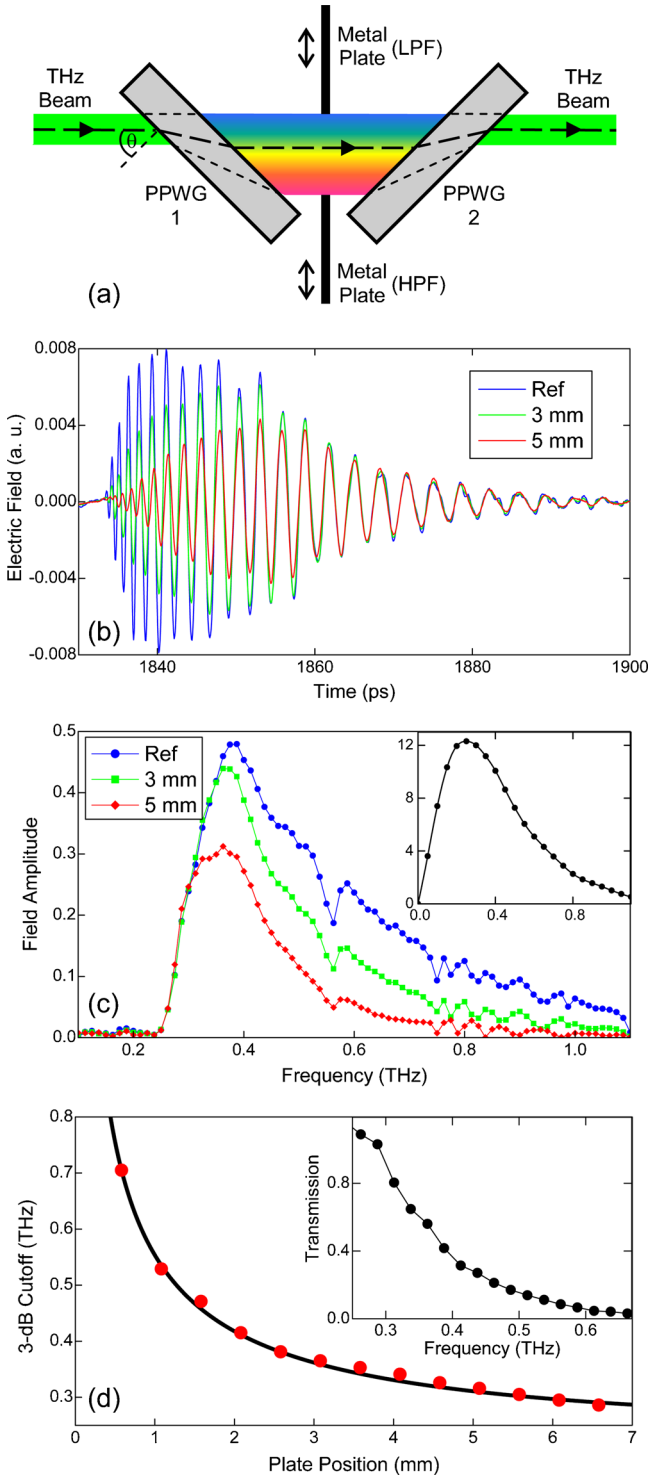

FIG. 1. (Color online) (a) The device geometry showing the two complementary PPWGs. The metal plates (beam blocks) used for the LPF and HPF are also shown. The spatial frequency spread is schematically indicated by the colors, where the high-frequency components are toward the blue side, while the low-frequency components are toward the red side. (b) Typical time-domain output signals for different positions of the metal plate in the *low-pass* configuration. The reference is when the beam between the PPWGs is unblocked. (c) Amplitude spectra corresponding to the waveforms in (b). The spectrum shown in the inset is when the device is not in the path of the beam. (d) Experiment (red dots) vs theory (black curve) comparing the 3 dB cutoff of the filter. Inset shows a typical experimental filter response indicating the low-pass behavior, when the plate moves in by 6 mm from the unblocked position.

a 12.7 mm waveguide length, and an incidence angle $\theta = 50°$ to achieve a sufficient frequency spread. In developing the theory, we assume that when the metallic plate is positioned with its edge located at the optic axis, it blocks half of the beam, and hence half of the power, compared to that of the unblocked reference signal. This is a reasonable assumption considering the spatial symmetry of the input Gaussian beam, which allows us to derive the theoretical 3 dB cutoff frequency as a function of the plate position. This theoretical dependence, which ignores possible diffractive effects, is shown in Fig. 1(d) along with the experimental values (red dots). In plotting the experimental values, we have adjusted the first data point (at 0.705 THz) to lie on the curve, with all the other points following accordingly. This point corresponds to the configuration of the beam least affected by the placement of the plate. This adjustment compensates for experimental uncertainty in the position of the input optic axis.

We can also demonstrate a tunable HPF by inserting a plate between the two PPWGs from the opposite side, starting from the low-frequency end [see Fig. 1(a)]. As the plate is inserted into the beam, it blocks frequency components starting from the low-end of the input spectrum. The lower-cutoff frequency of this HPF can be tuned by varying the plate position. Figure 2(a) shows typical time-domain output signals as the plate moves in by 6 and 8 mm from an unblocked (reference) position. Once again, the inherent negative chirp allows us to observe a progressive decrease in amplitude starting from the low-frequency end. The corresponding spectra shown in Fig. 2(b) confirm the high-pass behavior.

Similar to the LPF, we can determine the filter response [inset of Fig. 2(c)] and compare the experimental and theoretical 3 dB cutoff frequencies. This comparison is shown in Fig. 2(c) and also shows very good agreement. Here, the last data point (at 0.288 THz) is fit to the theoretical curve, and all other points follow accordingly. The experimental point used for the fit corresponds to the least affected beam configuration, and as above is necessary to compensate for uncertainty in the position of the input optic axis.

A key advantage of this filter design is its versatility. In addition to the low-pass and high-pass configurations shown in Figs. 1 and 2, we can just as easily switch to a band-pass or band-stop (or notch) filter. These results are summarized in Figs. 3(a) and 3(b), respectively. As shown in the insets, the band-pass configuration is realized by positioning a metallic *slit* between the two PPWGs, whereas the band-stop configuration is realized by positioning a metallic *strip* between the PPWGs. In both cases, the red trace shows the time-domain output signal, while the blue trace shows the unblocked (reference) signal. In Fig. 3(a), we observe a progressive decrease in amplitude going toward the leading (high-frequency) and trailing (low-frequency) ends of the signal from the center (mid-band), indicating a very clear band-pass behavior. The slight attenuation in the mid-band frequencies is caused by the relatively smaller 2.5 mm slit width, compared to the approximately 10 mm ($1/e$−amplitude) size of the input THz beam. In contrast, in Fig. 3(b), we observe a progressive decrease in amplitude going toward the center (mid-band) from the leading (high-frequency) and trailing (low-frequency) ends, indicating a clear band-stop behavior. Here, the strip width is 7 mm. If the width had been 10 mm, the same size as the input beam diameter, this would have represented a clear notch behavior

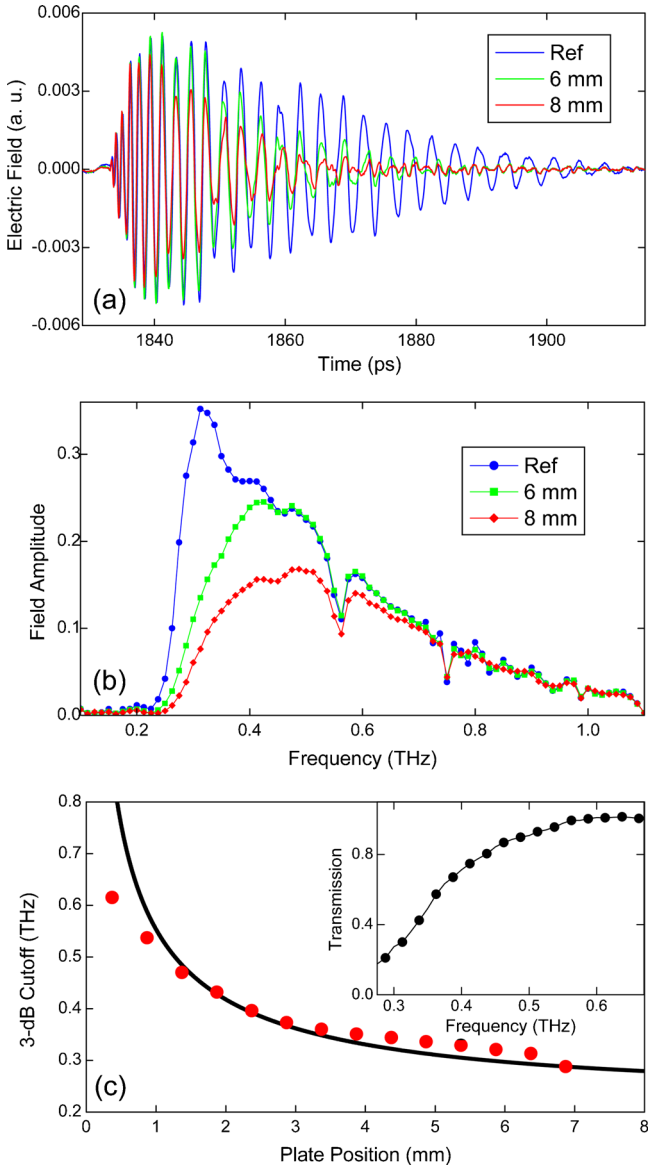

FIG. 2. (Color online) (a) Typical time-domain output signals for different positions of the metal plate in the *high-pass* configuration. The reference is when the beam between the PPWGs is unblocked. (b) Amplitude spectra corresponding to the waveforms in (a). (c) Experiment (red dots) vs theory (black curve) comparing the 3 dB cutoff of the filter. Inset shows a typical experimental filter response indicating the high-pass behavior, when the plate moves in by 7 mm from the unblocked position.

completely eliminating a "single" frequency. However, the larger width would also attenuate more of the neighboring high and low frequency components due to the spatially overlapping spectral content. To reduce this overlap, we can use a smaller input beam size or modify the design geometry to increase the degree of spatial chirp.

In conclusion, we have demonstrated a device that can be used as a tunable *universal* THz filter, which can provide the important signal-processing functionalities of low-pass, high-pass, band-pass, and band-stop (or notch) filtering. Other configurations such as comb filtering and phase (rather than amplitude) modulation are also possible, depending on the mask employed. We can even envision "THz pulse shaping" via the use of more complex amplitude and/or phase

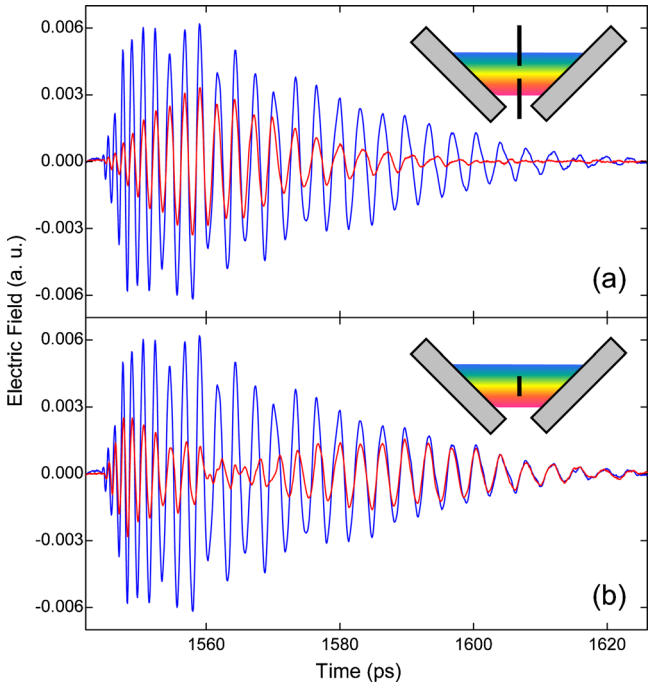

FIG. 3. (Color online) (a) Typical time-domain output signal (red) and reference (blue) in a *band-pass* configuration, where a metallic slit is positioned between the PPWGs as shown in the inset. (b) Typical time-domain output signal (red) and reference (blue) in a *band-stop (or notch)* configuration, where a metallic strip is positioned between the PPWGs as shown in the inset.

masks. As with well-known femtosecond optical pulse shapers, access to the spatially chirped THz beam affords a high degree of control of the output THz waveform and spectrum, and can therefore be important in a wide range of applications. This device concept can also be used to spatially separate, and then re-combine different THz frequencies, a multiplexing technique that could be called Frequency-Division-Spatial-Multiplexing (FDSM).

This work was supported in part by the National Science Foundation and by the Air Force Research Laboratory through the CONTACT program.

[1]R. Piesiewicz, T. Kleine-Ostmann, N. Krumbholz, D. Mittleman, M. Koch, J. Schöbel, and T. Kürner, IEEE Antennas Propag. Mag. **49**, 24 (2007).
[2]D. M. Mittleman, M. Gupta, R. Neelamani, R. G. Baraniuk, J. V. Rudd, and M. Koch, Appl. Phys. B: Lasers Opt. **67**, 379 (1999).
[3]T. D. Drysdale, I. S. Gregory, C. Baker, E. H. Linfield, W. R. Tribe, and D. R. S. Cumming, Appl. Phys. Lett. **85**, 5173 (2004).
[4]H. Nemec, P. Kuzel, L. Duvillaret, A. Pashkin, M. Dressel, and M. T. Sebastian, Opt. Lett. **30**, 549 (2005).
[5]C.-Y. Chen, C.-L. Pan, C.-F. Hsieh, Y.-F. Lin, and R.-P. Pan, Appl. Phys. Lett. **88**, 101107 (2006).
[6]J. W. Lee, M. A. Seo, D. J. Park, D. S. Kim, S. C. Jeoung, C. Lienau, Q.-H. Park, and P. C. M. Planken, Opt. Express **14**, 1253 (2006).
[7]M. A. Kaliteevski, S. Brand, J. Garvie-Cook, R. A. Abram, and J. M. Chamberlain, Opt. Express **16**, 7330 (2008).
[8]O. Paul, R. Beigang, and M. Rahm, Opt. Express **17**, 18590 (2009).
[9]R. Mendis and D. M. Mittleman, J. Opt. Soc. Am. B **26**, A6 (2009).
[10]R. Mendis and D. M. Mittleman, Opt. Express **17**, 14839 (2009).
[11]R. Mendis and D. Grischkowsky, Opt. Lett. **26**, 846 (2001).
[12]R. Mendis and D. M. Mittleman, IEEE Trans. Microwave Theory Tech. **58**, 1993 (2010).